

# Mesoscale Electric Power Generation From Pressurized Gas Flow

D. Krähenbühl<sup>1</sup>, C. Zwysig<sup>1</sup>, H. Weser<sup>2</sup> and J. W. Kolar<sup>1</sup>

<sup>1</sup>Power Electronic Systems Laboratory, ETH Zurich, Switzerland

<sup>2</sup>High Speed Turbomaschinen GmbH, Wolfsburg, Germany

**Abstract:** New ultra compact energy generation systems require increased speeds for higher power densities of the electrical machine and the turbomachinery. This paper presents a miniature compressed-air-to-electric-power system, based on a radial turbine with a rated rotational speed of 490 000 rpm and a rated electric power output of 150 W. A comprehensive description including turbine and diffuser, permanent magnet (PM) generator and power and control electronics is given and steps of future research are described.

**Key Words:** radial turbine, turbomachinery, ultra high speed

## 1. INTRODUCTION

In pressure reduction devices, such as valves, conventional throttles or turbo expanders, the excess process energy is usually wasted as heat. However this energy could be recovered by a system that removes the energy from pressurized gas flow and converts it into electrical energy. One example is the replacing of the throttle in automotive applications. There, a turbine with generator can replace the function of a conventional throttle and thereby produce a maximum electrical power of 1.5 kW [1]. In gas pipelines, energy can be recovered at pressure reduction stations if throttling valves are replaced by expanders driving electrical generators [2]. The power levels can be up to 1 MW, however, the pressure reduction process is usually done in several stages. Also, the turbo expanders nowadays used in cryogenics plants transfer the excess power (in the kW range) to a brake compressor where the energy is finally dissipated into cooling water. If the turbo expander was braked by a generator, the energy would be recovered, and therefore the efficiency of such plants could be increased.

Several of these applications, such as in automobiles, need ultra compact power generation systems. Power density in both turbomachinery and electrical machines increases with increasing rotational speed [3]. Therefore, these systems can have a speed between 100 000 rpm and 1 Mrpm at power levels of up to several kilowatts.

Besides higher power applications micro-turbines with less than 100 W power output and very high speeds have been reported in the literature. In [4], a modular system consisting of an air-turbine, a permanent-magnet (PM) generator and the power electronic controller has been designed, with a maximal power output of 1.1 W and a maximal speed of 200 000 rpm.

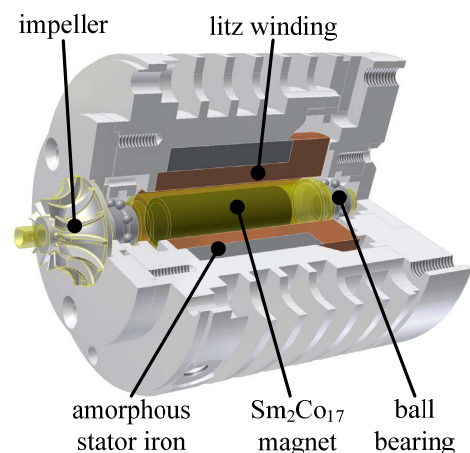


Fig. 1. Solid model of the turbo compressor system.  
Dimensions: 33 x 43mm.



Fig. 2. PM Generator with stator guide vanes and the radial-flow turbine ( $d = 10.5$  mm).

The off-the-shelf air turbine is taken from a dental drill. Drawbacks of this system are the poor power density ( $0.02 \text{ W/cm}^3$ ) and the large inlet flow rate of 45 l/min at maximum power output. In [5], a micro gas turbine coupled to a commercial electric machine with a maximal electric power output of 16 W at 160 000 rpm has been introduced for later use in a gas turbine system. This system achieves a power density of  $1.6 \text{ W/cm}^3$ , excluding power and control electronics.

In this paper, a compressed-air-to-electric-power system with a rotational speed of 490 000 rpm and a power output of 150 W is presented. The system is based on the reversal of an existing turbocompressor system, shown in Fig. 1. This turbocompressor reaches a maximal pressure ratio of 1.8 at a maximal rotational speed of 500 000 rpm and a power input of 150 W. It is driven by a low voltage electronics with 28 V dc input. With new and specially designed guide vanes, the turbo compressor system can be reversed and operated as a turbine system. This new, compressed-air-to-electric-power system comprises of an inward-flow radial (IFR) turbine (Fig. 2), a PM generator and the power and control electronics as detailed in the following.

## 2. SYSTEM INTEGRATION

For the existing turbo compressor system, a detailed electromagnetic machine design, on analysis of the mechanical stresses and rotor dynamics, and a thermal design has already been made. These design considerations are also valid for the compressed-air-to-electric-power system and only parts of the hardware have to be modified.

The output of the new system is controlled to 24 V dc, facilitating easier application than the variable dc output voltage in [4] and the variable three phase ac voltages in [5]. Furthermore, an increased power density is achieved. The PM generator with turbine has a volume of  $36.8 \text{ cm}^3$  ( $d = 3.3 \text{ cm}$   $l = 4.3 \text{ cm}$ ) and the electronics interface has a volume of  $60.8 \text{ cm}^3$  ( $l = 4.5 \text{ cm}$ ,  $b = 4.5 \text{ cm}$ ,  $h = 3 \text{ cm}$ ). This leads to a generator power density of  $4 \text{ W/cm}^3$  and of  $1.5 \text{ W/cm}^3$  including the power and control electronics.

## 3. ELECTRICAL CONSIDERATIONS

The rotor of the PM generator consists of a diametrically magnetized cylindrical  $\text{Sm}_2\text{Co}_{17}$  permanent magnet encased in a retaining titanium sleeve ensuring sufficiently low mechanical stresses on the magnet. The eccentricity is minimized by shrink fitting the sleeve on the permanent magnet and grinding the rotor. Due to its simplicity and small size the PM generator utilizes two high-speed ball bearings. The stator magnetic field rotates with high frequency (8.3 kHz), it is therefore necessary to minimize the losses in the stator core by using amorphous iron. In order to minimize the eddy current losses in the three-phase air-gap copper winding, the winding is realized with litz-wire. Considering the magnet flux linkage  $\Psi_{PM}$  the motor has a peak phase-to-phase voltage of 19.4 V at 490 000 rpm. The length of the shaft is adjusted such that rated speed falls between the second and the third bending modes. The measured machine

efficiency  $\eta_{mr}$  at rated power output is 87 % including air friction and bearing losses. A detailed description of the generator has been presented in [6] and in Table I the measured electrical data of the PM motor is summarized.

The bi-directional power electronics consists of an active 3-phase rectifier and an additional boost converter and has been analyzed in [7]. The power electronics have an efficiency of 95 % at rated power.

Table I

electrical data	
rated speed $n_r$	490 000 rpm
rated electric output $P_{el}$	150 W
magnet flux linkage $\Psi_{PM}$	0.22 mVs
back EMF at rated speed	11.2 V
stator inductance $L_S$	2.25 $\mu\text{H}$
stator resistance $R_S$	0.125 $\Omega$
machine efficiency $\eta_{mr}$	87 %
power electronics efficiency $\eta_{el}$	95 %
thermodynamic data	
inlet temperature $T_0$	300 K
inlet pressure $p_0$	3.5 bar
outlet pressure $p_2$	1.12 bar
guide vane efficiency $\eta_n$	90.25 %
isentropic efficiency $\eta_{is}$	70 %
turbine data	
effective turbine inlet area $A_1$	17 $\text{mm}^2$
effective turbine exit area $A_2$	19.5 $\text{mm}^2$

## 4. TURBOMACHINERY CONSIDERATIONS

The system was originally designed as a turbo compressor. Therefore the dimensions of the rotor are given, especially the inlet and outlet angle of the rotor blades. For this reason, the stator guide vanes have to be adjusted to meet optimum efficiency at a rated rotational speed of 490 000 rpm. Since the inlet angle of the turbine blade is zero, the relative velocity  $w_1$  has to be orthogonal to the rotational speed  $u_1$  (Fig. 4a). In the following analysis it can be assumed that the compressed air behaves like a perfect gas, i.e.  $h = c_p T$ . The complete adiabatic expansion process for a turbine is represented by the enthalpy entropy diagram (equivalent to the temperature entropy diagram) shown in Fig. 3. The ideal enthalpy change ( $\Delta h_s$ ), i.e. the ideal or reversible expansion, is in between the inlet and outlet pressure, but at constant entropy (line 0 – 1<sub>s</sub> – 2<sub>s</sub>). Assuming adiabatic flow through the turbine, the corresponding temperature drop  $\Delta T_s$  can be calculated with

$$\Delta T_{(0-2s)} = T_0 \left( 1 - \frac{p_0}{p_2} \left( \frac{1}{\kappa} - 1 \right) \right) = 83.4 \text{ K} \quad (1)$$

$$T_{2s} = T_0 - \Delta T_{(0-2s)} = 216.6 \text{ K} \quad (2)$$

where  $\kappa$  is the specific heat ratio. The actual expansion follows the line 0 - 1 - 2, the temperature drop  $\Delta T_2$  can be calculated with the isentropic efficiency  $\eta_{is}$ ,

$$\Delta T_2 = \Delta T_{(0-2s)} \eta_{is} = 58.4 \text{ K} \rightarrow T_2 = 241.6 \text{ K} \quad (3)$$

In an adiabatic turbomachine work done determines the change of enthalpy. The losses are uniquely caused by the increase of entropy of the fluid.

The temperature  $T_1$  in between stator and rotor can be calculated via the specific kinetic energy of the absolute velocity at rotor entry  $c_1$

$$\Delta T_{(0-1s)} = \frac{c_1^2}{2c_p \eta_n} = 44.4 \text{ K} \quad (4)$$

$$\Delta T_{(0-1)} = \Delta T_{(0-1s)} \eta_n = 40.1 \text{ K} \quad (5)$$

where  $c_p$  is the specific heat capacity. As a result of miniaturization, and therefore a larger influence of side friction, the guide vane efficiency  $\eta_n$  has to be determined with measurements. However, the guide vane efficiency was assumed to be about 90 %.

The pressure  $p_1$  in between the stator and rotor can now be calculated with

$$p_1 = p_0 \left( 1 - \frac{\Delta T_{(0-1s)}}{T_0} \right)^{\frac{\kappa}{\kappa-1}} = 2 \text{ bar.} \quad (6)$$

In Fig. 5 the layout of the stator and the rotor is plotted. From the rotor inlet ( $r_3$ ) the rotor blades extend radially inward and turn the flow into the axial direction. The exit part of the blades is curved to remove the absolute tangential component of velocity. In Fig. 4b the velocity diagram for the turbine outlet is drawn. The air gap between the radial turbine and the spiral casing has to be as thin as possible, in order to minimize the tip leakage losses. The constant mass flow rate through the turbine can be written as

$$\dot{m} = \delta_1 c_{r1} A_1 = \left( \frac{p_1}{RT_1} \right) c_{r1} A_1 = 4 \frac{\text{g}}{\text{s}} \quad (7)$$

where  $R$  is the ideal gas constant. The effective turbine inlet area  $A_1$  also accounts for the rotor blade thickness. The maximum output power of the turbine can now be calculated with

$$P = \dot{m}(u_1 c_{\theta 1} - u_2 c_{\theta 2}) = \dot{m} \cdot u_1^2 = 291 \text{ W} \quad (8)$$

where  $c_{\theta 1} = u_1$  and  $c_{\theta 2} = 0 \frac{\text{m}}{\text{s}}$ . From this value, the leakage losses, as well as the side friction of the turbine disk back are deducted, these values will be determined experimentally. Furthermore, the known machine and power electronics efficiencies must be considered.

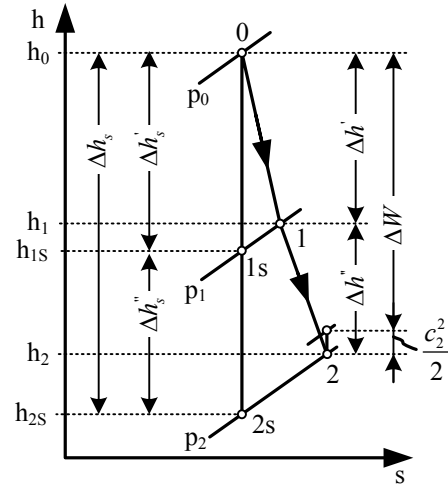


Fig. 3. Enthalpy entropy diagram (*hs*-diagram) specific work:  $\Delta W = u_1 c_{\theta 1} - u_2 c_{\theta 2}$ .

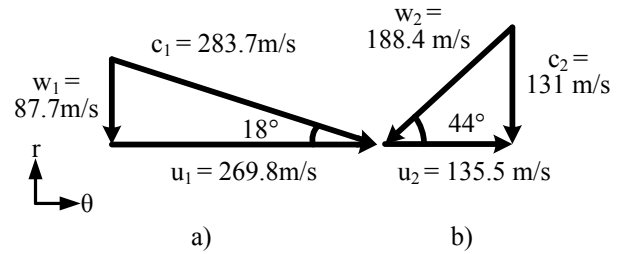


Fig. 4. Velocity diagrams at rotor entry (a) and outlet (b) for the rated rotational speed.  $c_1/c_2$  absolute velocity at rotor inlet/outlet.  $w_1/w_2$  relative velocity at rotor inlet/outlet.  $u_1/u_2$  stator speed at radius  $r_3$  and  $\bar{r}_{4,5}$ .

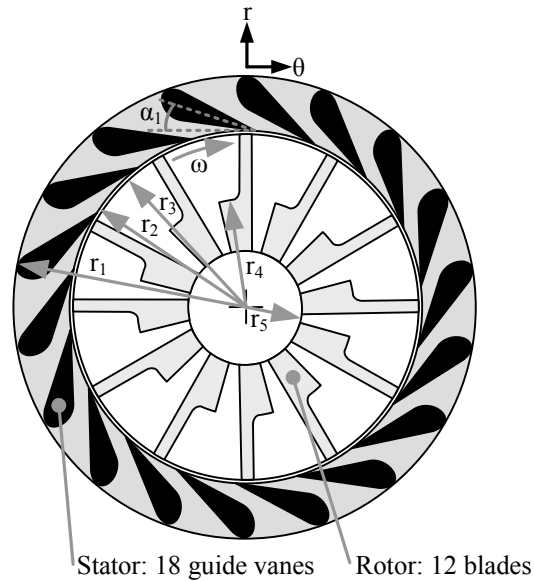


Fig. 5. Radial flow turbine ( $r_1$ : 7 mm,  $r_2$ : 5.335 mm,  $r_3$ : 5.25 mm,  $r_4$ : 3.3 mm,  $r_5$ : 1.75 mm,  $\alpha_1$ : 18°).

Including all these losses, the target electric power output is 150 W.

## 5. TEST BENCH

An experimental test bench is built in order to verify theoretical considerations and the compressed-air-to-power system concept. Therefore, a mass flow sensor and several thermocouple and pressure sensors are used. The generator has been tested as a motor up to a speed of 550 000 rpm and the total rated losses in the stator core (0.5 W), the copper losses in the winding (5 W), air friction losses due to windage (6 W) and the ball bearing friction losses where measured (8 W).

## 6. FUTURE STEPS

In a first step the aerodynamic performance, e.g. the theoretical turbine-map, the efficiency and the computed data, will be experimentally verified. There, for a better specification of the overall efficiency, especially the turbine leakage losses must be measured, because of the high ratio between turbine air gap and turbine diameter.

In a next step, the assembly of an ultra compact (20 x 50 mm) air-to-power demonstrator, with a compressed air input of 3 to 8 bar, and electrical output of 100 W, will be developed. The rated speed for the turbine and generator will be 350 000 rpm. The device must be able to follow load changes; therefore the mass flow will be controlled with a high-speed on/off valve, by using PWM control technique.

In Fig. 6 the solid model of the air-to-power demonstrator is shown. The pressurized air inlet is located at the right side of the system. The air flow gets accelerated and diverted from the diffuser, so that the relative velocity at the axial turbine entry is equivalent to the turbine inlet angle. At the turbine outlet the air has a pressure of approximately one bar, is radially diverted and leaves the system. The cold outlet air stream can be used for cooling, particularly for the machine and the power electronics.

The assembly of the generator is identical to the system described in section 3. Since the rated speed of the new air-to-power system is less than the 500 000 rpm, the generator design has to be optimized again, considering the total losses [8].

## 7. CONCLUSION

This paper shows how an existing high-speed turbo compressor system is reversed to a compressed-air-to-power system. Even though the described system is not optimized concerning high power density and high efficiency, the computed values are significantly higher compared to similar systems described in the literature.

Due to the miniaturization, the guide vane efficiency and the isentropic efficiency can not be predicted analytically and have to be determined experimentally.

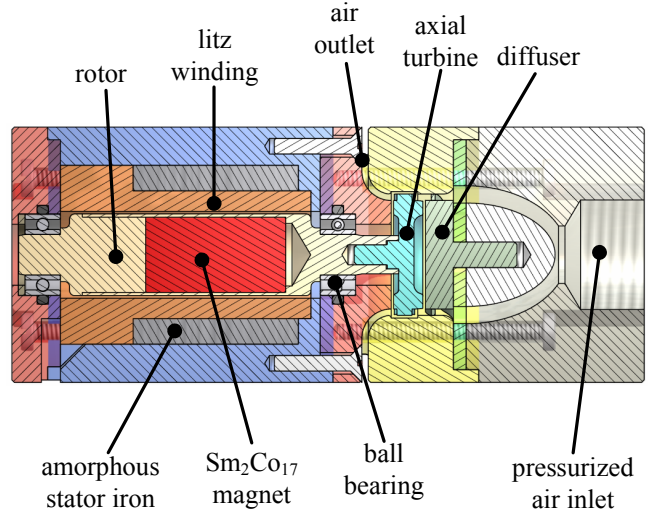


Fig. 6 Solid model of the ultra compact (20 x 50 mm) air-to-power demonstrator.

## REFERENCES

- [1] L. Guzzella, M. Betschart, T. Fluri, R. De Santis, C. Onder, T. Auckenthaler, "Recuperative Throttling of SI Engines for Improved Fuel Economy", SAE 2004 World Congress & Exhibition, March 2004, Detroit, MI, USA.
- [2] A. Mirandola and L. Minca, "Energy Recovery by Expansion of High Pressure Natural Gas", Proc. of the 21st Intersociety Energy Conversion Engineering Conference, Vol. 1, pp. 16-21, San Diego, California, Aug. 25-29, 1986.
- [3] A. Binder, T. Schneider, "High-Speed Inverter-Fed AC Drives," International Aegean Conference on Electrical Machines and Power Electronics, Electromotion 2007, Bodrum, Turkey, Sept. 10-12, 2007.
- [4] D.P. Arnold, P. Galle, F. Herrault, S. Das, J.H. Lang, and M.G. Allen, "A Self-Contained, Flow-Powered Microgenerator System", PowerMEMS05, Tokyo.
- [5] J. Peirs, D. Reynaerts, F. Verplaetsen, "A Microturbine for Electric Power Generation", Sensors and Actuators A: Physical Volume 113, Issue 1, 15 June 2004, pp. 86-93
- [6] C. Zwyszig, J.W. Kolar, "Design Considerations and Experimental Results of a 100 W, 500 000 rpm Electrical Generator", Journal of Micromechanics and Microengineering, Issue 9, pp. 297 - 302, Sept. 2006.
- [7] C. Zwyszig, S.D. Round and J.W. Kolar, "Power Electronics Interface for a 100 W, 500 000 rpm Gas Turbine Portable Power Unit," Applied Power Electronics Conference, Dallas, Texas, USA, March 19-23, pp. 283-289, 2006.
- [8] J. Luomi, C. Zwyszig, A. Looser, and J.W. Kolar, "Efficiency Optimization of a 100-W, 500 000-rpm Permanent-Magnet Machine Including Air Friction Losses," in *IEEE Industry Applications Conference 2007*, New Orleans, USA, 2007.